Atmos. Chem. Phys. Discuss., https://doi.org/10.5194/acp-2019-292
Manuscript under review for journal Atmos. Chem. Phys.
Discussion started: 29 April 2019

Atmospheric Chemistry and Physics Discussions

Enhanced sulfate formation through SO_2+NO_2 heterogeneous reactions during heavy winter haze in the Yangtze River Delta region, China

Ling Huang[1+], Jingyu An[2+], Bonyoung Koo[3], Greg Yarwood[4], Rusha Yan[2], Yangjun Wang[1], Cheng Huang[2*], Li Li[1*]

[1]School of Environmental and Chemical Engineering, Shanghai University, Shanghai, 200444, China
[2]State Environmental Protection Key Laboratory of the Cause and Prevention of Urban Air Pollution Complex, Shanghai Academy of Environmental Sciences, Shanghai, 200233, China
[3]Bay Area Air Quality Management District, San Francisco, 94105, USA
[4]Ramboll, Novato, California, 95995, USA

[+]These two authors contributed equally to this work.

Correspondence to: Li Li (lily@shu.edu.cn) and Cheng Huang (huangc@saes.sh.cn)

Abstract. Rapid sulfate formation is recognized as key characteristics of severe winter haze in China. However, air quality models tend to underestimate sulfate formation during heavy haze periods and heterogeneous formation pathways have been proposed as promising mechanisms to reduce gaps between observation and model simulation. In this study, we implemented a reactive SO_2 uptake mechanism through the SO_2 + NO_2 heterogeneous reactions in the Comprehensive Air Quality Model with extensions (CAMx) to improve simulation of sulfate formation in the Yangtze River Delta (YRD) region for the first time. Parameterization of the SO_2 + NO_2 heterogeneous reactions is based on observations in Beijing and considered both impact of relative humidity and aerosol pH on sulfate formation. Ammonia is reported to be critical for the formation of secondary inorganic aerosols and estimation of ammonia emissions is usually associated with large uncertainties. Sensitivity tests were conducted to evaluate the importance of the SO_2 + NO_2 heterogeneous reactions as well as ammonia emissions on modelled sulfate concentrations during a period with several heavy haze episodes in the YRD region. Base case model results show large underestimation of sulfate concentrations by 36 % under polluted conditions in the YRD region. Adding the SO_2 + NO_2 heterogeneous reactions or doubling ammonia emissions alone leads to slight model improvement (~6 %) on simulated sulfate concentrations in the YRD region. However, model performance significantly improved when both the SO_2 + NO_2 heterogeneous reactions and doubled ammonia emissions were included in the simulation: predicted sulfate concentrations during polluted periods increased from 23.1 μg m^{-3} in the base scenario to 29.1 μg m^{-3} (representing an increase of 26 %). Aerosol pH is crucial for the SO_2 + NO_2 heterogeneous reactions and our calculated aerosol pH is always acidic and increased by 0.7 with doubled ammonia emissions. Modelling results also show that this reactive SO_2 uptake mechanism enhanced sulfate simulations by 1 to 5 μg m^{-3} for the majority of eastern and central part of China, with more than 20 μg m^{-3} increase of sulfate concentrations over the north-eastern plateau. These findings

suggest that the SO_2 + NO_2 heterogeneous reactions could be important for sulfate formation in the YRD region as well as other parts of China. In addition, ammonia emissions need to be carefully estimated. More studies are needed to improve the parameterization of the SO_2 + NO_2 heterogeneous reactions based on local data further evaluate this mechanism in other regions. Substantial efforts are needed to improve the accuracy of ammonia emissions inventory.

1 Introduction

Rapid sulfate (SO_4^{2-}) formation has been reported to be key characteristics of severe winter haze in China. However, most air quality models tend to underestimate sulfate formation during severe winter haze episodes in China because standard SO_2 oxidation pathways, including gas-phase chemistry (i.e. oxidized by hydroxyl radical OH) and aqueous-phase chemistry (i.e. oxidized by ozone (O_3), hydrogen peroxide (H_2O_2)) are suppressed by weak photochemical activity and low ozone concentrations (Quan et al., 2014)). Meanwhile, analysis of severe haze events in China show enhanced secondary inorganic aerosols, especially sulfate concentrations. For example, Quan et al. (2014) found that observed sulfate accounted for 13 % of $PM_{2.5}$ (particulate matter with dynamic equivalent diameter less than 2.5 μm) on normal clean days and increased to 25 % on haze days during the infamous 2013 January Beijing haze period. For the same haze episode, Cheng et al. (2016) used concentration ratios of sulfate to sulfur dioxide ($[SO_4^{2-}]/[SO_2]$) to diagnose sulfate production rate; this ratio increased with $PM_{2.5}$ levels and was 6 times higher under the most polluted conditions than normal conditions. Most current air quality models (e.g. CMAQ, GEOS-Chem, WRF-Chem, CAMx), which only include the traditional gaseous- or aqueous-phase mechanisms for sulfate formation, do not show very good model performances of sulfate concentrations against observations during haze periods in China (Wang et al., 2014; Zheng et al., 2015; Gao et al., 2016a, 2016b; Li et al., 2015). The under-prediction of sulfate concentrations could be related to uncertainties of the emissions inventory, bias of simulated meteorological fields, and/or some missing sulfate formation mechanisms that are not included in the current models.

Heterogeneous sulfate production chemistry has been proposed by several studies to explain the high concentrations and rapid formation of sulfate during haze episode in China (e.g. He et al., 2014; Wang et al., 2014; Zheng et al., 2015; Wang et al., 2016; Cheng et al., 2016; Guo et al., 2017). He et al. (2014) suggested a synergistic effect between NO_2 and SO_2 on the surface of mineral dust (i.e. mineral oxides) as an important source of sulfate in China and emphasized the essential role of O_2 involved in this process. More generally, heterogeneous loss of SO_2 on aerosol surfaces (not limited to mineral dust) or deliquescent aerosols is discussed by many studies, although the exact underlying mechanism is still unknown (e.g. Wang et al., 2014; Zheng et al., 2015). For this kind of heterogeneous reactions, the sulfate production rate has been parameterized as a pseudo first-order reaction with respect to the gaseous SO_2 concentration with the SO_2 reactive uptake coefficient (γ) on aerosol surfaces being the key parameter. This uptake coefficient, representing the probability that a SO_2 gas molecule colliding with an aerosol surface results in sulfate formation, is reported to be heavily dependent on relative humidity (RH) (Zheng et al., 2015; Wang et al., 2016). Parameterized reactive uptake of SO_2 has been implemented in several current air quality models, including GEOS-Chem, WRF-Chem, CMAQ and CAMx, and generally improved model performance of

sulfate concentrations during haze episodes in China (e.g. Wang et al., 2014; Zheng et al., 2015; Gao et al., 2016b). Two more recent papers, Wang et al. (2016) and Cheng et al. (2016) further suggested that reaction between NO_2 and SO_2 in aerosol water may contribute substantially to sulfate formation during haze events in China. Both studies emphasized the importance of higher aerosol pH (5.4–6.2 reported by Cheng and 6.0–7.6 by Wang) sustained by abundant gas-phase ammonia (NH_3) during haze periods being an essential precondition for this mechanism. However, the near-neutralized aerosol pH that facilities SO_2 oxidation by NO_2 is questioned by Guo et al. (2017) who concluded from a thermodynamic analysis that aerosol pH was always acidic (4.5–5) regardless of the ambient NH_3 concentrations and that the NO_2-mediated oxidation of SO_2 was unlikely to be important in China or any other region of the world. Guo et al. (2017) pointed out that within low pH ranges (up to 4.5), SO_2 oxidation catalyzed by transition metal (i.e. Fe(III) and Mn(II)) might become a dominant sulfate formation pathway in aerosol water and suggested it as an alternative to SO_2 + NO_2 reactive uptake as being a potential sulfate contributor under haze conditions. Most recently, Song et al. (2018) suggested the heterogeneous hydroxymethanesulfonate (HMS) chemistry being a potentially important contributor to heavy haze pollution in northern China. Hung et al. (2018) reported the interfacial SO_2 oxidation on the surface of aqueous micro-droplets as a potential pathway to explain fast conversion of SO_2 to sulfate.

To investigate whether the SO_2 + NO_2 reactions in aerosol water could help better predict the enhanced sulfate formation during haze periods in the Yangtze River Delta (YRD) region, we implemented a parameterized SO_2 + NO_2 reactive uptake mechanism in the Comprehensive Air Quality Model with Extensions (CAMx), which is a widely used air quality model in China (e.g. Wang et al., 2009; Huang et al., 2012; Li et al., 2013, 2015; Jia et al., 2017; etc.). Our parameterization specifically incorporated RH and aerosol pH dependencies derived from measurement data during the 2015 Beijing haze event (Wang et al., 2016). Although the RH dependency of the SO_2 uptake rate has already been implemented in previous studies (e.g. Zheng et al., 2015; Wang et al., 2014), the effect of aerosol pH has not been explicitly included in any modelling studies yet to our knowledge. Another highlight of this study is that while most of the previous studies were trying to improve model predictions in the northern part of China, especially the Beijing-Tianjin-Hebei region (e.g. Gao et al., 2016b; Zheng et al., 2015), this work is the first study to focus on the Yangtze River Delta region, which has also suffered from severe haze problems in recent years due to urban expansion and industrialization (e.g. Li et al., 2011; M. Wang et al., 2015; Xu et al., 2016; Ming et al., 2017). In addition to the SO_2 + NO_2 heterogeneous reactions, we also investigated model sensitivities to ammonia emissions, which have been reported to be crucial for the formation of secondary inorganic aerosols and large uncertainties exist with current ammonia emission inventory (Huang et al., 2011; Fu et al., 2013).

2 Methodology

2.1 SO_2 + NO_2 mechanism in CAMx

In this study, we implemented the SO_2 + NO_2 reactive uptake mechanism in CAMx version 6.40 (Ramboll Environ, 2016) as a pseudo gas-phase reaction:

Atmos. Chem. Phys. Discuss., https://doi.org/10.5194/acp-2019-292
Manuscript under review for journal Atmos. Chem. Phys.
Discussion started: 29 April 2019

Atmospheric Chemistry and Physics Discussions

$$SO_2 + NO_2 \xrightarrow{k_{het}} SO_4^{2-} \quad (1)$$

Since the vapor pressure of sulfuric acid is very low, we assumed all sulfuric acid partitions to the aerosol phase. The rate constant k_{het} is related to the reactive uptake coefficient γ for SO_2 as follows:

$$\frac{d[SO_4^{2-}]}{dt} = k_{het}[NO_2(g)][SO_2(g)] = \frac{1}{4}\gamma\bar{C}S[SO_2(g)] \quad (2)$$

where $\bar{C}$ is the mean molecular speed (m/s), and S is the aerosol surface area concentration (m^2/m^3). Based on the observations during the Chinese haze events (Wang et al., 2016), this uptake coefficient γ depends on aerosol pH, RH, and NO_2 concentration. Therefore, we assumed a functional form of γ as the product of each of these dependencies:

$$\gamma = 4k_0 d_f [NO_2(g)] \quad (3)$$

where d_f is the pH-dependent distribution factor of SO_2, i.e. the ratio of SO_2 concentration in the aqueous-phase to the gaseous-phase; k_0 (ppm^{-1}) is the RH-dependent parameter; $NO_2(g)$ is the NO_2 gas concentration. We used the data in Table S2 and S4 of Wang et al. (2016) to back calculate the RH dependency of k_0 under clean (observed sulfate concentration less than 10 μg m^{-3}), transition (sulfate between 10 and 20 μg m^{-3}), and polluted (sulfate more than 20 μg m^{-3}) conditions during Beijing 2015 episodes. Aerosol pH was calculated using the ISORROPIA thermodynamic equilibrium model implemented in CAMx assuming a metastable aerosol liquid phase which is an appropriate assumption for most ambient conditions including the Chinese haze events (Guo et al. 2017). Wang et al (2016) only reported NOx (not NO_2) concentrations in Beijing during the 2015 haze event. We simply assumed a NO_2/NOx ratio of 0.5. Inserting NO_2 concentrations, γ values from Wang et al. (2016), and calculated aerosol pH from ISORROPIA into Eq. 3, we obtained the expression of k_0 depending upon RH as follows (parameters for k_0 calculation is shown in Table S1):

$$k_0 = \begin{cases} \text{RH<21\%:} & 199.25 \\ \text{21\%≤RH<41\%:} & (284.22-199.25)\text{x}(\text{RH-21\%})/(41\%-21\%)+199.25 \\ \text{41\%≤RH<56\%:} & (322.16-284.22)\text{x}(\text{RH-41\%})/(56\%-41\%)+284.22 \\ \text{RH≥56\%:} & 332.16 \end{cases} \quad (4)$$

The rate constant k_{het} of SO_2 + NO_2 is formulated as:

$$k_{het} = k_0 d_f \bar{C} S \quad (5)$$

SO_2 lifetime (in hr) associated with the SO_2 + NO_2 reactive uptake mechanism is calculated as:

$$SO_2\ lifetime = \frac{1}{k_{net}[NO_2(g)]} \quad (6)$$

Figure 1 shows the SO_2 lifetime as a function of aerosol pH for clean, transition, and polluted conditions, with other variables kept constant. The SO_2 lifetime shortens as aerosol pH becomes more neutralized, indicating faster conversion of SO_2 to sulfate by SO_2 + NO_2 reactive uptake on aerosol. For pH within 2 to 7, one unit increase in aerosol pH shortens SO_2 lifetime by about one order of magnitude. The blue, orange, and red symbols in Figure 1 correspond to the clean, transition, and polluted conditions during Beijing 2015 based on data in Table S1. As shown in Figure 1, the aerosol pH values

calculated by ISORROPIA are 5.5 (for clean conditions) and 4.1-4.2 (for transition and polluted conditions), all lower than the values (7.6) reported by Wang et al. (2016). As noted by Guo et al. (2017), it is important to make a consistent assumption for aerosol state (i.e., metastable) in deriving and implementing the parameterization for reactive uptake. A most recent paper by Song et al (2018) identified coding errors with the ISORROPIA model, which resulted unrealistic pH values of 7.7 using the standard ISORROPIA model with the stable state assumption in previous studies. Nevertheless, our results are not compromised by this coding error because the metastable assumption was chosen in our ISORROPIA calculation.

2.2 Model configuration

Two versions of the Comprehensive Air Quality Model with extensions (CAMx) modified based on the original version 6.40 (Ramboll Environ, 2016) were used in this study: one with the SO_2 + NO_2 heterogeneous reactions (described in Section 2.1) and one without (forcing k_{het} equals to zero). The modeling domain consists of three nested grids (Figure 2): the outer 36 km domain (D01) covers most of China, Japan, Korea, parts of India, and southeast Asia; the 12 km domain (D02) covers eastern China and the inner 4 km domain (D03) covers Shanghai, Jiangsu province, Zhejiang province, Anhui province, and parts of surrounding provinces, together referred as the Yangtze River Delta (YRD) region. Meteorological fields were based on simulation results from the Weather Research and Forecasting (WRF) model (version 3.7) driven by the National Centers for Environmental Prediction (NCEP)/National Center for Atmospheric Research (NCAR) Operational Global Analysis data (http://dss.ucar.edu/datasets/ds083.2/). Details of the WRF configurations can be found in previous studies (Liu et al., 2018). Boundary conditions for D01 were generated from the Model for OZone And Related chemical Tracers (MOZART) global chemistry model (Emmons et al., 2010). The Carbon Bond 6 (CB6) mechanism (Yarwood et al., 2010) was used for the gas phase chemistry and the static two-mode coarse/fine (CF) scheme was used to represent particle size distribution. The Zhang dry deposition (Zhang et al. 2003) and default wet deposition scheme was used to for removal processes. Anthropogenic emissions for areas outside the YRD region were from the Multi-resolution Emission Inventory for China (MEIC, http://www.meicmodel.org/). For emissions within the YRD region, an YRD-specific emission inventory (Huang et al., 2011; Li et al., 2011) was updated to year 2014 and utilized in this study. Biogenic emissions were simulated using the Model of Emissions of Gases and Aerosols from Nature (MEGAN, version 2.1, Guenther et al. 2012) based on the WRF simulation results. The modeling episode is December 2013, during which several heavy haze events with hourly $PM_{2.5}$ concentration higher than 500 μg m^{-3} were observed in the YRD region.

Four simulations with identical model configuration and input data including meteorology, initial/boundary conditions, and emission inventory (except ammonia emissions) were conducted using the above two different CAMx versions:

– noHet (base case): simulation based on CAMx version without the SO_2 + NO_2 heterogeneous reactions (this is also our base case). Note that this CAMx version differs from the distributed CAMx v6.40 in that we removed the original heterogeneous sulfate formation reaction which only included a simple parameterization based on RH (Zheng et al. 2015) in the distributed version. This is done on purpose to quantify the influence of the newly parameterized SO_2 + NO_2 heterogeneous reactions on sulfate formation.

- Het: simulation based on CAMx with the SO_2 + NO_2 heterogeneous reactions. Other model configurations were identical to scenario noHet.
- noHet_2NH_3: CAMx version and model configurations were same as scenario noHet except ammonia emissions were doubled for the 4 km domain.
- Het_2NH_3: CAMx version and model configurations were same as scenario Het but ammonia emissions were doubled for the 4 km domain.

We first ran CAMx for 36 km/12 km domains with two-way nested; for the 4 km domain, we used boundary conditions extracted from the 12 km model outputs and conducted the above four scenarios. Fourteen vertical layers were used extending from the surface to 100 mb. In addition to default CAMx outputs, we modified the source code to generate additional diagnostic variables (e.g. aerosol pH, RH, and k_{het}) to evaluate the SO_2 + NO_2 heterogeneous reactions.

2.3 Observations

Hourly observations of ozone, SO_2, NO_2, $PM_{2.5}$ and its components including sulfate, nitrate, ammonium, organic carbon (OC), and elemental carbon (EC) are available between 1 December and 29 December 2013 at a monitor site located at the center of the urban area of Shanghai (referred as SAES site, 31.1695°N, 121.4305°E, Figure 3). Hourly $PM_{2.5}$ observations are also available at another 23 monitor sites across the YRD region (Figure 3; see locations in Table S2). During this period, YRD region experienced relative clean days as well as several heavy haze episodes with peak $PM_{2.5}$ exceeding 600 μg m^{-3} during a most heavily polluted period of December 5th to 7th. At the SAES site, maximum hourly $PM_{2.5}$ concentration reached 540.3 μg m^{-3} on December 6th with a monthly average of 118.7 μg m^{-3}. We followed the method in Wang et al (2016) to divide the period into clean (observed sulfate <10 μg m^{-3}), transition (10-20 μg m^{-3}), and polluted (>20 μg m^{-3}) periods based on observed hourly sulfate concentration at the SAES site. Compared with clean period, all PM species increased by more than 3 times (sulfate, nitrate and ammonium (SNA) increase by more than 5 times) during polluted period as indicated by the enhancement ratio (calculated as the ratio of average concentrations during the polluted period divided by those during the clean period). In terms of fraction of $PM_{2.5}$, SNA increased from 44 % during clean period to 69 % during polluted period while carbonaceous aerosols (OC and EC) decreased from 32 % to 24 %. This is consistent with the commonly observed characteristics of winter haze periods in China reported by many previous studies (e.g. Wang et al., 2014; Zheng et al., 2015; Cheng et al., 2015) that SNA is playing a more important role during the heavy haze periods. Average sulfate concentration of clean, transition and polluted periods was 6.7, 14.2, and 36.1 μg m^{-3}, respectively, accounting for 17-23 % of $PM_{2.5}$ (Figure S1).

Observations of ambient ammonia concentrations are also available at the SAES site; however, the quality of measurements is questionable. Therefore, we used ammonia observations from a similar urban site nearby (referred as FDU site, ~15 km north from the SAES site, 31.3005°N, 120.9778°E, Figure 3) for analysis in this study. Observations at the FDU site have been discussed by S. Wang et al. (2015) and demonstrated data reliability. Diurnal NH_3 concentrations at the FDU site during our modeling period showed a weak bimodal pattern with an average of 7.3 ppb (ranging 1.6–25 ppb) during this

period (Figure S2). This two-peak diurnal variation is caused by vehicle emissions and evolution of the boundary layer (S. Wang et al. 2015). In summary, observations for gases species (except NH_3) and PM species at the SAES site and NH_3 at the FDU site were used for model validation in this study.

2.4 Statistical metrics for model validation

For WRF and CAMx model performance valuation, mean bias (MB), normalized mean bias (NMB), and index of agreement (IOA) were used in this study. Calculations of these selected metrics are shown below:

$$MB = \frac{1}{N}\sum(P_j - O_j) \quad (6)$$

$$NMB = \frac{\sum(P_j - O_j)}{\sum O_j} \times 100 \quad (7)$$

$$IOA = 1 - \frac{\sum(P_j - O_j)^2}{\sum(|P_j - \bar{O}| + |O_j - \bar{O}|)^2} \quad (8)$$

where P_j and O_j are predicted and observed hourly concentrations or values, respectively. N is the number of paired model and observation data. $\bar{O}$ is the average concentration/value of observations. IOA ranges from 0 to 1 with 1 indicating perfect agreement between model and observation.

3 Results and discussions

3.1 Model evaluation

3.1.1 WRF results evaluation

Model performance of WRF results is generally acceptable in this study. Table S3 summarizes the meteorological performance statistics of WRF during December 2013 at Pudong and Hongqiao airport stations in Shanghai (Figure 3). All meteorological parameters were well reproduced with NMB and NME within 37% and 42%, respectively; IOA values are above or close to 0.8. Bias of predicted wind speed is within 0.31 degree. Comparisons of hourly observed and simulated relative humidity, wind speed and temperature at these two stations suggest reasonable model results in terms of temporal variations (Figure S3). Overall, the WRF simulated results are acceptable to be used in subsequent CAMx simulations.

3.1.2 CAMx base scenario (noHet) evaluation

Figure 4 depicts the time series of simulated and observed concentrations for sulfate and $PM_{2.5}$ during 1 to 29 December 2013 at SAES site (see Figure S4 in Supplemental Information for other species). Overall, the model is successful in capturing the temporal variations of ozone and PM species with IOA values above 0.5 (Table S4). For sulfate, the model captured the day-to-day sulfate variations reasonably well with an overall MB of -2.8 μg m^{-3} and IOA of 0.80. For clean and transition periods, model showed slight over-prediction with MB of 1.1 and 0.5 μg m^{-3} (Table S5). However, during

polluted period when observed sulfate concentrations are higher than 20 μg m^{-3}, model significantly underestimated sulfate formation with a MB of -13.0 μg m^{-3} (NMB of -36 %). Observed maximum sulfate concentration reached 93.4 μg m^{-3} but model only predicted 52.2 μg m^{-3}. Nitrate and ammonium concentrations were also underestimated by 20 % on average and exacerbated to more than 40 % during polluted periods. For carbonaceous aerosols, elemental carbon (EC) was underestimated by 32 % while organic carbon (OC) exhibited even more underestimation of almost 50 %. Underestimation of OC is usually associated with underestimation of secondary organic aerosols (SOA). Discussion of OC under-prediction is beyond the scope of current work and will be addressed in future studies. Results of the four CAMx simulations in this study showed negligible changes in predicted EC/OC concentrations and thus are excluded in the following discussions.

Figure 5 depicts the averaged $PM_{2.5}$ during the modeling episode over the YRD region with observations at 24 monitoring sites. Observed $PM_{2.5}$ concentrations generally showed a decreasing trend from north to south of the YRD region, which was well captured by the model. For sites located in southern Jiangsu and southern Zhejiang province, the model showed favorable agreement with the observations. Underestimations existed for sites located in the northern part of Jiangsu and Zhejiang province. MB across all 24 monitoring sites ranged from as low as -90.4 μg m^{-3} (site in north Jiangsu province) to slight overestimation of 11.4 μg m^{-3} (site in south Zhejiang province); corresponding NMB ranged from -46 % to 16 % (Table S2).

3.2 Simulated PM concentrations at SAES site

3.2.1 Sulfate concentrations

Four scenarios – noHet, Het, noHet_2NH_3 and Het_2NH_3 were conducted to evaluate the impact of the SO_2 + NO_2 heterogeneous reactions and ammonia emissions on sulfate simulation. We first analyzed the modeled results at the SAES site; then we discussed the spatial patterns over the YRD region. Table 1 shows the average sulfate concentration for different scenarios by clean, transition, and polluted periods; corresponding scatter plots are shown in Figure 6. A complete summary of statistical metrics for each scenario/period is presented in Table S5.

Impact of SO_2 + NO_2 heterogeneous reactions (noHet vs. Het)

As shown in Figure 6, simulated sulfate concentrations compared well with observations under clean and transition conditions in the noHet scenario with over-prediction by 16 % and 4 %, respectively. By contrast, large under-prediction of sulfate concentration existed during polluted periods (MB of -13.0 μg m^{-3}, NMB of -36 %). Adding the SO_2 + NO_2 heterogeneous reactions showed small enhancement on sulfate formation, reducing the overall NMB from -16 % to -12 %. If only polluted periods are considered, simulated sulfate concentrations increased from 23.1 to 24.6 μg m^{-3} with the heterogeneous reactions, corresponding to an increase by 6.5 %. Thus even with the SO_2 + NO_2 heterogeneous reactions, model was still under-predicting sulfate concentrations on heavy haze days with a NMB of -32 %. This is because aerosol pH was always acidic (pH < 3; this will be discussed in the following section) and the SO_2 + NO_2 heterogeneous reactions were not being appreciable within this pH range (Figure 1). Model performances for clean and transition periods were

slightly compromised with the SO_2 + NO_2 heterogeneous reactions since the base scenario was already overestimating sulfate concentrations.

Impact of NH_3 emissions (noHet vs. noHet_2NH_3)

Being the dominant base gas in the atmosphere, ammonia plays an essential role in the formation of secondary inorganic aerosols and estimation of ammonia emissions is usually associated with large uncertainties (e.g. Huang et al., 2011; Fu et al., 2013). With the base case ammonia emissions, NH_3 concentration was under-predicted by 3.0 ppb (NMB of -60 %). With doubled ammonia emissions, ammonia concentration was over-predicted by 1.7 ppb with NMB of 34 %. NMB of sulfate concentrations during polluted period is -32 %, which is similar to the enhancement caused by that of the SO_2 + NO_2 heterogeneous reactions. Clearly, doubling ammonia emissions is not enough to close the gap between observed and simulated sulfate concentrations during heavy haze periods. We performed additional sensitivity tests with even higher ammonia emissions and found that 10 times ammonia emissions would be needed to achieve an average sulfate concentration (33.2 μg m^{-3}) that is comparable with observation (36.1 μg m^{-3}) under polluted conditions (with no heterogeneous reactions). However, in that case, model performance of ammonia is significantly compromised with over-prediction by 32.3 ppb. These results indicate that the uncertainties associated with the ammonia emissions are not enough to fully explain the under-prediction of sulfate formation during heavy haze periods in the YRD region.

Impact of both (noHet vs. Het_2NH_3)

A fourth scenario (Het_2NH_3) with the SO_2 + NO_2 heterogeneous reactions as well as doubled ammonia emissions gave the best model performance of sulfate concentrations with an overall MB of -0.2 μg m^{-3} (NMB of -1 %, Figure 6). During polluted periods, average sulfate concentration was predicted to be 29.1 μg m^{-3} (representing an increase of 26% from the base case) and NMB was reduced from -36 % in the base scenario to -19 % in the Het_2NH_3 scenario. Maximum sulfate concentration simulated under scenario Het_2NH_3 was 97.2 μg m^{-3}, which compared well with the observed maximum of 93.4 μg m^{-3} at the SAES site. With doubled ammonia emissions, the heterogeneous reactions were playing an increasing important role in sulfate formation by boosting average sulfate concentrations from 24.5 (noHet_2NH_3) to 29.1 μg m^{-3} (Het_2NH_3) under polluted conditions, representing an increase by 19 %. This is because aerosol pH was elevated by ~0.7 with more ammonia available and the rate of the heterogeneous reactions is positively correlated with aerosol pH (Figure 1). These results indicate that the SO_2 + NO_2 heterogeneous reactions as well as sufficient ammonia emissions are both needed to greatly improve model simulation of sulfate formation under polluted conditions. However, it is to mention that model performance under clean and transition periods got compromised most under scenario Het_2NH_3.

Figure 7 shows a Q-Q plot of modeled versus observed sulfate concentrations for the four scenarios. Underestimations of sulfate concentrations become noticeable around 35 μg m^{-3} in all scenarios and between 35 to 55 μg m^{-3}, there appears to be a systematical low bias in predicted sulfate concentrations that neither doubled ammonia emissions nor the heterogeneous reactions or both could stimulate notable sulfate formation. Scenario Het_2NH_3 gives the best model performance with an overall MB of -0.2 μg m^{-3} but still underpredicts sulfate formation under heavy haze periods by -19 %. This could be related to still biased ammonia emissions, less direct emissions of sulfate and/or SO_2, and/or missing of other sulfate formation

pathways that needs further investigation. Another explanation is that the SO_2 + NO_2 heterogeneous reactions implemented in this study were parameterized based on observations in Beijing but the simulation is performed over the YRD region. It would be ideal to use local observations for model parameterization in future studies.

Sulfate formation under selected episodes

We further selected four heavy haze episodes (EP1-EP4) with observed sulfate concentrations continuously exceeding 30 μg/m^3 (as highlighted in Figure 4) at the SAES site. These episodes lasted from 9 hours (EP2) to as long as 37 hours (EP1). Episode average sulfate concentrations are all above 50 μg m^{-3} (Figure S5) except for EP3 (36.2 μg m^{-3}). It is interesting to note that for all selected episodes except EP3, sulfate formation was enhanced in scenario Het_2NH$_3$ by 10.4 to 14.6 μg m^{-3} while EP3 only exhibits minimal increase of modeled sulfate concentrations by only 0.8 μg m^{-3}. We performed additional sensitivity tests and found that even with 10 times ammonia emissions, modeled sulfate concentration during EP3 is enhanced by only 2.3 μg m^{-3}, which is still much lower compared to the observed values. We suspect that other factors, for example, meteorology might be biased during EP3 and lead to the underpredicted sulfate concentrations. Another explanation for the almost unchanged modeled sulfate concentration during EP3 is that we used SO_2 emission inventory of year 2014 for the simulation of 2013 December. It is possible that SO_2 emissions of year 2014 are lower than the level in 2013 due to SO_2 reduction policies implemented in the YRD region. When EP3 is excluded, modeled sulfate concentrations during heavy pollution episodes are greatly enhanced from 33.5 μg m^{-3} in the base scenario to 46.2 μg m^{-3} in scenario Het_2NH$_3$ (increase by 38 %), due to the combined influences of the SO_2 + NO_2 heterogeneous reactions and doubled ammonia emissions.

3.2.2 Nitrate and ammonium concentrations

In addition to sulfate, we also look at modeled nitrate and ammonium concentrations under different scenarios; associated model performance metrics are summarized in Table S6 and S7. For the base case scenario, nitrate and ammonium concentrations were underestimated by 20 %. When only polluted period is considered, underestimation almost doubled to 36 % and 41 % for nitrate and ammonium, respectively. Doubling ammonia emissions results in higher nitrate concentrations simply because more ammonia becomes available to form nitrate. This reduces nitrate underestimation substantially during polluted period from -42 % to -20 % but also leads to even higher nitrate overestimation during clean and transition periods but. The impact of the SO_2 + NO_2 heterogeneous reactions on nitrate formation, on the other hand, is more complicated. With the base case ammonia emissions, predicted nitrate concentrations show negligible changes with the implementation of the heterogeneous reactions. However, with doubled ammonia emissions, predicted nitrate formation is enhanced by 0.3–1.1 μg m^{-3} (noHet_2NH$_3$ vs. Het_2NH$_3$). Response of simulated nitrate concentrations to the SO_2 + NO_2 heterogeneous reactions, in other words, to increased sulfate concentrations, could be affected by two opposing factors. At one hand, nitrate concentrations decrease due to replacement by enhanced formation of sulfate. On the other hand, nitrate formation could be enhanced with more effective hydrolysis of N_2O_5 on sulfate aerosols (Hallquist et al., 2003). A most recent study by Vasilakos et al. (2018) discussed the nitrate substitution paradox with less sulfate and concludes that this

paradox is attributable to positive bias in model simulated aerosol pH. Nevertheless, compared with doubled ammonia emissions, the heterogeneous reactions only had small impact on modeled nitrate concentration.

For ammonium, doubling ammonia emissions also leads to higher simulated ammonium concentrations but to a less extent compared with nitrate. Under-prediction of ammonium under polluted conditions is reduced from 41 % in the base case to 31 % in the noHet_2NH_3 scenario. With the base case ammonia emissions, adding the SO_2 + NO_2 heterogeneous reactions leads to slight increase in ammonium concentrations. When ammonia emissions are doubled, the heterogeneous reactions substantially improve modeled ammonium concentrations. Overall MB of ammonium in scenario Het_2NH_3 is only -0.4 μg m^{-3} (NMB of -3 %) and under-prediction during polluted period is reduced to 24 % in the Het_2NH_3 scenario (from 41 % in the base case scenario). These results suggest that both the heterogeneous reactions as well as sufficient ammonia emissions are needed to improve model simulation of ammonium concentrations.

3.2.3 $PM_{2.5}$ concentrations

In the base case scenario, $PM_{2.5}$ concentrations are underestimated by 36 % at the SAES site during polluted periods (Table S8). With doubled ammonia emissions, $PM_{2.5}$ under-prediction is reduced to 30 % during polluted periods, resulting an overall NMB of -2 %. $PM_{2.5}$ concentrations do not change much with the heterogeneous reactions when ammonia emissions are at base case level. With doubled ammonia emissions, concentrations of all three inorganic species are enhanced with the heterogeneous reactions; thus under-prediction of $PM_{2.5}$ during polluted periods in scenario Het_2NH_3 is further reduced to 26 % and the overall NMB is only 1 %. The maximum of simulated $PM_{2.5}$ concentration increases from 460.6 μg m^{-3} in the base scenario to 531.6 μg m^{-3} in scenario Het_2NH_3 (increase by 15 %), which compares well with observed maximum value of 540.3 μg m^{-3}.

3.3 Predicted aerosol pH at the SAES site

Aerosol pH, which is calculated from ISORROPIA within CAMx, is crucial for the heterogeneous SO_2 + NO_2 reactions to be effective. Figure 8 shows the distribution of modeled aerosol pH at the SAES site by scenario/period. In general, aerosol is predicted to be more acidic as pollution develops. Average modeled aerosol pH for clean, transition, and polluted period of the base scenario (noHet) is 2.8, 2.6, and 2.3, respectively. This is consistent with the higher SO_2 concentrations observed under polluted conditions (Figure S6). Maximum aerosol pH reached 5.0, 4.4, and 3.8 under clean, transition and polluted periods in the base scenario. When NH_3 emissions are doubled, averaged aerosol pH increases by ~0.7 to 3.0–3.5; maximum aerosol pH during clean, transition and polluted periods is 5.7, 5.1, and 4.2 under scenario noHet_2NH_3. Adding the SO_2 + NO_2 reactions (i.e. scenario Het) slightly decreases the aerosol pH by 0.03–0.12, with stronger reduction associated with more enhancement of sulfate formation. These results indicate that aerosol pH at the SAES site is always acidic and increasing ammonia emissions could raise aerosol pH by some extent. A possible explanation for the pH differences seen between the acidic ranges in this study and more neutralized values reported in previous studies for the Beijing-Tianjin-Hebei region (e.g. 5.4 to 6.2 reported by Cheng and 6.0 to 7.6 by Wang, the latter was later found to be associated with a

coding bug in ISORROPIA) might be due to lower ammonia levels in Shanghai compared with Beijing (S. Wang et al. 2015). However, even when ammonia emissions are increased by 10 times, maximum aerosol pH value is predicted to be 4.8 under polluted condition, which is still lower than the values reported for north China. Our results seem to be consistent with the conclusion of Guo et al. (2017) that aerosol pH is always acidic regardless of the ambient ammonia concentrations.

3.4 Spatial impact of the SO_2 + NO_2 heterogeneous reactions and ammonia emissions in YRD region

Figure 9 shows the spatial distribution of monthly mean sulfate, nitrate, ammonium, and $PM_{2.5}$ concentrations simulated in the base case and the differences between base case and other three sensitivity runs in the YRD region. Similar plots of ammonia, SO_2 and aerosol pH are shown in Figure S7. Overall, impacts of the heterogeneous reactions and ammonia emissions over the YRD region are similar to that observed at the SAES site. With the SO_2 + NO_2 heterogeneous reactions only, predicted monthly mean sulfate concentrations show ubiquitous increase of 0.1–5 μg m^{-3} across the domain with larger increase observed in the north and northwest directions. Regions with relative higher increase of predicted sulfate concentrations closely track regions with relatively high aerosol pH (Figure S7). For nitrate concentrations, however, the heterogeneous reactions lead to increase in the northwest region but decrease for the rest of the YRD region. Magnitudes of changes in nitrate concentrations in both directions are within 1 μg m^{-3}. Predicted ammonium concentrations show less than 1 μg m^{-3} increase over the majority of the domain. Domain average $PM_{2.5}$ concentrations increased by 1.2 μg m^{-3} with spatial patterns similar to sulfate. Aerosol pH decreases slightly because more SO_2 is pulled into the aerosol phase.

With doubled ammonia emissions, predictions of all three inorganic PM species are enhanced with most profound impacts observed for nitrate. Uniform increase across the YRD region is observed for predicted sulfate concentrations; for nitrate and ammonium, increase of predicted concentrations is more significant towards the south. Domain averaged sulfate, nitrate, ammonium and $PM_{2.5}$ concentrations increase by 0.5, 6.2, 0.3, and 8.0 μg m^{-3}, respectively. Aerosol pH is also elevated (on average by 0.3) with more ammonia available. In south Anhui and south Zhejiang provinces, elevation of aerosol pH exceeds one unit. Areas with larger pH increase are also areas with relatively lower pH values in the base scenario, indicating that aerosol pH responds nonlinearly to ammonia emissions.

When both the heterogeneous reactions and doubled ammonia emissions are considered, simulated sulfate concentrations are enhanced by 2.7 μg m^{-3} across the YRD region. Minimal changes in nitrate and ammonium concentrations are observed with and without the heterogeneous reactions when ammonia emissions are doubled. For $PM_{2.5}$, domain average concentrations increase by 11.6 μg m^{-3}. Simulated $PM_{2.5}$ concentrations show better agreement with observations at the 24 monitoring sites (Figure 5); averaged NMB is reduced from -21 % in the base scenario to -11 % in scenario Het_2NH_3.

3.5 Simulated sulfate concentrations over China

Figure 10 compares the average simulated sulfate concentrations between the base case and Het scenario for the outer 36 km domain during the modelling period. In the base case simulation, high sulfate concentrations were noticed at scattered cities over the North China Plain, Central China and the central part of the Sichuan Basin. Implementing the SO_2 + NO_2

heterogeneous reactions enhanced simulated sulfate concentrations by at least 1~5 μg m^{-3} for regions to the east of the "Hu Line". In particular, Northeast China Plain shows most significant sulfate enhancement of more than 10 μg m^{-3}; simulated average sulfate concentrations of the Het scenario exceed 30 μg m^{-3}. For regions that show relative high sulfate concentrations in the base case scenario, sulfate concentrations were increased by 5-10 μg m^{-3} due to the implementation of the reactive SO_2 uptake mechanism. The spatial pattern of sulfate enhancement generally follows that of ammonia concentrations (Figure S8), once again suggesting the important role of ammonia emissions for this mechanism. Future studies and local sulfate observations are needed to further evaluate this mechanism for other parts of China, especially for Northeast China Plain.

4 Conclusions

In this study, we implemented a new parameterization of the SO_2 + NO_2 heterogeneous reactions based on observations in Beijing to improve model simulation of sulfate formation under heavy haze conditions in the YRD region. Unlike previous studies that only considered the influence of relative humidity on sulfate formation, we also included the impact of aerosol pH in our parameterization. Four CAMx sensitivity runs were conducted to evaluate the importance of the SO_2 + NO_2 heterogeneous reactions as well as ammonia emissions on simulated sulfate concentrations in the YRD region. Base case simulation showed reasonable model performance of sulfate with an overall MB of -2.7 μg m^{-3} but significantly underpredicted sulfate concentrations by 36 % during polluted conditions. Implementation of the SO_2 + NO_2 heterogeneous reactions alone showed slight improvement of sulfate simulation (increase by 6.5 %) under polluted conditions due to acidic aerosol pH. Doubling ammonia emissions alone exhibited a similar impact (sulfate increase by 5.6 %) with that of the SO_2 + NO_2 heterogeneous reactions alone. Nevertheless, aerosol pH increased by 0.7 with doubled ammonia emissions, which enabled the SO_2 + NO_2 heterogeneous reactions to become effective. Thus, in a fourth scenario where both the SO_2 + NO_2 heterogeneous reactions and doubled ammonia emissions were considered, simulated sulfate concentrations during polluted periods increased from 23.1 μg m^{-3} in the base case to 29.1 μg m^{-3}, representing an increase by 26 %. Results for sulfate simulations over entire China shows that for some parts of China, especially the Northeast China Plain, implementing the SO_2 + NO_2 heterogeneous reactions could lead to as much as 20 μg m^{-3} increase of sulfate concentrations and the spatial pattern of sulfate enhancement follows closely to that of ammonia concentrations. These findings suggest that the SO_2 + NO_2 heterogeneous reactions could be important for sulfate formation under heavy haze periods and aerosol pH (in other words, ammonia emissions) is crucial in this process. However, under-prediction of sulfate concentration still exists (by 20 %) in the YRD region under polluted conditions even with the SO_2 + NO_2 heterogeneous reactions and doubled ammonia emissions, which urges further efforts to better constrain the parameterization of the SO_2 + NO_2 heterogeneous reactions using local data and to improve the accuracy of ammonia emissions inventory.

Date and code availability. All data and modified CAMx code is available upon request from the corresponding authors.

Competing interest. The authors declare that they have no conflict of interest.

Special issue statement. This article is part of the special issue "Multiphase chemistry of secondary aerosol formation under severe haze". It is not associated with a conference.

Author contribution. L.H., J.A., L.L., C.H. and G.Y. designed the research; B.K. and L.H. modified the code; R.Y. conducted WRF simulation; J.A. conducted CAMx simulations; L.H. and J.A. analyzed the data; L.L., G.Y., C.H. and Y.W. provided important academic guidance; L.H. and J.A. wrote the paper with contributions from all authors.

Acknowledgement. This study was financially sponsored by the Shanghai Sail Program (NO. 19YF1415600), the National Natural Science Foundation of China (NO. 41875161), and Chinese National Key Technology R&D Program (NO. 2014BAC22B03 and NO. 2018YFC0213800). We thank Qi Zhang, Qian Wang, and Hongli Li from Shanghai University for helping with the data analysis.

References

Cheng, Y., Zheng, G., Wei, C., Mu, Q., Zheng, B., Wang, Z., Gao, M.,Zhang, Q., He, K.,Carmichael, G., Pöschl1, U., and Su, H.: Reactive nitrogen chemistry in aerosol water as a source of sulfate during haze events in China, Science Advances., 2, e1601530-e1601530, doi:10.1126/sciadv.1601530, 2016.

Emmons, L. K., Walters, S., Hess, P. G., J.-F., L., Pfister, G. G., Fillmore, D., Granier, C., Guenther, A.,Kinnison, D., Laepple, T.,Orlando, J., Tie, X., Tyndall, G., Wiedinmyer, C., Baughcum, S. L., and Kloster, S.: Description and evaluation of the model for ozone and related chemical tracers, version 4 (mozart-4), Geoscientific Model Development., 3, 43-67, doi:10.5194/gmd-3-43-2010, 2010.

Fu, X., Wang, S., Zhao, B., Xing, J., Cheng, Z., Liu, H., and Hao, J.: Emission inventory of primary pollutants and chemical speciation in 2010 for the Yangtze River Delta region, China, Atmos. Environ.., 70, 39-50, doi:39-50.10.1016/j.atmosenv.2012.12.034, 2013.

Gao, M., Carmichael, G. R., Wang, Y., Ji, D., Liu, Z., and Wang, Z.: Improving simulations of sulfate aerosols during winter haze over Northern China: the impacts of heterogeneous oxidation by NO_2, Frontiers of Environmental Science & Engineering., 10, 16, doi:10.1007/s11783-016-0878-2, 2016.

Gao, M., Carmichael, G. R., Wang, Y., Saide, P. E., Yu, M., Xin, J., Liu, Z., and Wang, Z.: Modeling study of the 2010 regional haze event in the North China Plain, Atmos. Chem. Phys., 16, 1673-1691.doi:10.5194/acpd-15-22781-2015, 2016.

Guenther, A. B., Jiang, X., Heald, C. L., Sakulyanontvittaya, T., Duhl, T., Emmons, L. K., and Wang, X.: The Model of Emissions of Gases and Aerosols from Nature version 2.1 (MEGAN2.1): an extended and updated framework for modeling biogenic emissions, Geoscientific Model Development., 5, 1471-1492, doi:10.5194/gmd-5-1471-2012, 2012.

Guo, H., Weber, R. J., and Nenes, A.: High levels of ammonia do not raise fine particle pH sufficiently to yield nitrogen oxide-dominated sulfate production, Scientific Reports., 7, 12109, doi:10.1038/s41598-017-11704-0, 2017.

Hallquist, M., Stewart, D. J., Stephenson, S. K., and Cox, R. A.: Hydrolysis of N_2O_5 on sub-micron sulfate aerosols, Physical Chemistry Chemical Physics., 5, 3453-3463. doi:10.1039/B301827J, 2003.

He, H., Wang, Y., Ma, Q., Ma, J., Chu, B., Ji, D.,Tang, G., Liu, C., Zhang, H., and Hao, J.: Mineral dust and NOx promote the conversion of SO_2 to sulfate in heavy pollution days, Scientific Reports., 4, 4172, doi:10.1038/srep04172, 2014.

Huang, Q., Cheng, S., Li, J., Chen, D., Wang, H., and Guo, X.: Assessment of PM_{10} emission sources for priority regulation in urban air quality management using a new coupled MM5-CAMx-PSAT modeling approach, Environmental Engineering Science., 29, 343-349, doi:http://doi.org/10.1089/ees.2011.0229, 2012.

Hung, H. M., Hsu, M. N., and Hoffmann, M. R.: Quantification of SO_2 Oxidation on Interfacial Surfaces of Acidic Micro-Droplets: Implication for Ambient Sulfate Formation, Environmental Science & Technology., 52, 9079-9086, doi:10.1021/acs.est.8b01391, 2018.

Jia, J., Cheng, S., Liu, L., Lang, J., Wang, G., Chen, G., and Liu, X.: An Integrated WRF-CAMx Modeling Approach for Impact Analysis of Implementing the Emergency $PM_{2.5}$ Control Measures during Red Alerts in Beijing in December 2015, Aerosol and Air Quality Research., 17, 2491-2508, doi:10.4209/aaqr.2017.01.0009, 2017.

Li, L., Chen, C. H., Fu, J. S., Huang, C., Streets, D. G., Huang, H. Y., Zhang, G. F., Wang, Y. J., Jang, C. J., Wang, H. L., Chen, Y. R., and Fu, J. M.: Air quality and emissions in the Yangtze River Delta, China, Atmos, Chem. Phys., 11, 1621-1639, doi:10.5194/acpd-10-23657-2010, 2011.

Li, L., An, J. Y., Zhou, M., Yan, R. S., Huang, C., Lu, Q., Lin, L., Wang, Y. J., Tao, S. K., Qiao, L. P., Zhu, S. H., and Chen, C. H.: Source apportionment of fine particles and its chemical components over the Yangtze River Delta, China during a heavy haze pollution episode, Atmos. Environ.., 123, 415-429, doi:10.1016/j.atmosenv.2015.06.051, 2015.

Li, L., Cheng, S., Li, J., Lang, J., and Chen, D.: Application of MM5-CAMx-PSAT Modeling Approach for Investigating Emission Source Contribution to Atmospheric Pollution in Tangshan, Northern China, Mathematical Problems in Engineering., 2013, 1-12, doi:10.1155/2013/136453, 2013.

Liu, Y., Li, L., An, J., Huang, L., Yan, R., Huang, C., Wang, H., Wang, Q., Wang, M., and Zhang, W.: Estimation of biogenic VOC emissions and its impact on ozone formation over the Yangtze River Delta region, China, Atmos. Environ.., 186, 113-128, doi:10.1016/j.atmosenv.2018.05.027, 2018.

Ming, L., Ling, J., Li, J., Fu, P., Yang, W., Di, L., Gan, Z., Wang, Z., and Li, X.: $PM_{2.5}$ in the Yangtze River Delta, China: Chemical compositions, seasonal variations, and regional pollution events, Environ. Pollut., 223, 200-212, doi:10.1016/j.envpol.2017.01.013, 2017.

Quan, J., Tie, X., Zhang, Q., Liu, Q., Li, X., Gao, Y., and Zhao, D.: Characteristics of heavy aerosol pollution during the 2012-2013 winter in Beijing, China, Atmos. Environ.., 88, 83-89, doi:10.1016/j.atmosenv.2014.01.058, 2014.

Ramboll Environ. User's Guide Comprehensive Air Quality Model with Extensions Version 6.40, 2016 December

Song, S., Gao, M., Xu, W., Sun, Y., Worsnop, D. R., Jayne, J. T., Zhang, Y., Zhu, L., Li, M., Zhou, Z., Cheng, C., Lv, Y., Wang, Y., Peng, W., Xu, X., Lin, N., Wang, Y., Wang, S., Munger, J. W., Jacob, D., and McElroy, M, B.: Possible heterogeneous hydroxymethanesulfonate (HMS) chemistry in northern China winter haze and implications for rapid sulfate formation, Atmos. Chem. Phys. Discuss., doi:10.5194/acp-2018-1015, 2018.

Vasilakos, P., Russell, A., Weber, R., and Nenes, A.: Understanding nitrate formation in a world with less sulfate, Atmospheric Chemistry and Physics, 18, 12765-12775, doi: 10.5194/acp-18-12765-2018, 2018.

Wang, G., Zhang, R., Gomez, M. E., Yang, L., Zamora, M. L., Hu, M., Lin, Y.,Peng, J., Guo, S., Meng J and Li, J.: Persistent sulfate formation from London Fog to Chinese haze, Proceedings of the National Academy of Sciences., 113, 13630-13635, doi:10.1073/pnas.1616540113, 2016.

Wang, M., Cao, C., Li, G., and Singh, R. P.: Analysis of a severe prolonged regional haze episode in the Yangtze River Delta, China, Atmos. Environ., 102, 112-121, doi;10.1016/j.atmosenv.2014.11.038, 2015.

Wang, S., Nan, J., Shi, C., Fu, Q., Gao, S., Wang, D., Cui, H., Saiz-Lopez.,and Zhou, B.: Atmospheric ammonia and its impacts on regional air quality over the megacity of Shanghai, China, Scientific reports., 5, 15842, doi:10.1038/srep15842, 2015.

Wang, Y., Zhang, Q., Jiang, J., Zhou, W., Wang, B., He, K., Duan, F.,Zhang, Q., Philip, S.,and Xie, Y.: Enhanced sulfate formation during China's severe winter haze episode in January 2013 missing from current models, Journal of Geophysical Research: Atmospheres., 119, 10425-10440, doi:10.1002/2013jd021426, 2014.

Wang, X., Li, J., Zhang, Y., Xie, S., and Tang, X.: Ozone source attribution during a severe photochemical smog episode in Beijing, China, Science in China Series B: Chemistry, 52, 1270-1280, doi:10.1007/s11426-009-0137-5, 2009.

Xu, J. S., Xu, H. H., Xiao, H., Tong, L., Snape, C. E., Wang, C. J., and He, J.: Aerosol composition and sources during high and low pollution periods in Ningbo, China, Atmos. Res., 178-179, 559-569, doi:10.1016/j.atmosres.2016.05.006, 2016.

Yarwood, G., J. Jung, G. Z. Whitten, G. Heo, J. Mellberg and E. Estes.: Updates to the Carbon Bond Mechanism for Version 6 (CB6), Presented at the 9th Annual CMAS Conference, Chapel Hill, October, 2010.

Zhang, L., Brook, J. R., and Vet, R.: A revised parameterization for gaseous dry deposition in air-quality models, Atmospheric Chemistry and Physics, 3, 2067-2082, doi:10.5194/acp-3-2067-2003, 2003.

Zheng, B., Zhang, Q., Zhang, Y., He, K. B., Wang, K., Zheng, G. J., Duan, F, K., Ma, Y, L., and Kimoto, T.: Heterogeneous chemistry: a mechanism missing in current models to explain secondary inorganic aerosol formation during the January 2013 haze episode in North China, Atmos. Chem. Phys., 15, 2031-2049, doi:10.5194/acp-15-2031-2015, 2015.

Atmos. Chem. Phys. Discuss., https://doi.org/10.5194/acp-2019-292
Manuscript under review for journal Atmos. Chem. Phys.
Discussion started: 29 April 2019

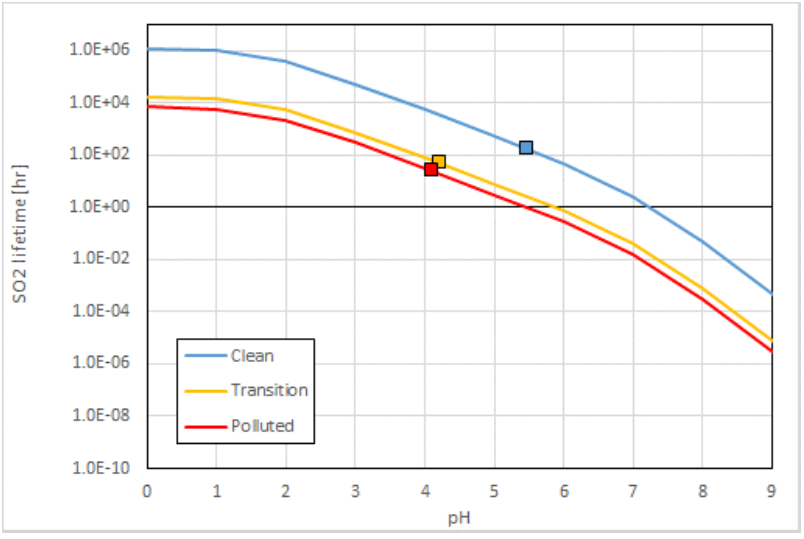

Figure 1: SO_2 lifetime (in hr^{-1}) due to SO_2 + NO_2 reactive uptake mechanism as a function of aerosol pH under clean, transition, and polluted conditions. Values of relative humidity, temperature, and NO_2(g) concentrations are based on values in Table S1.

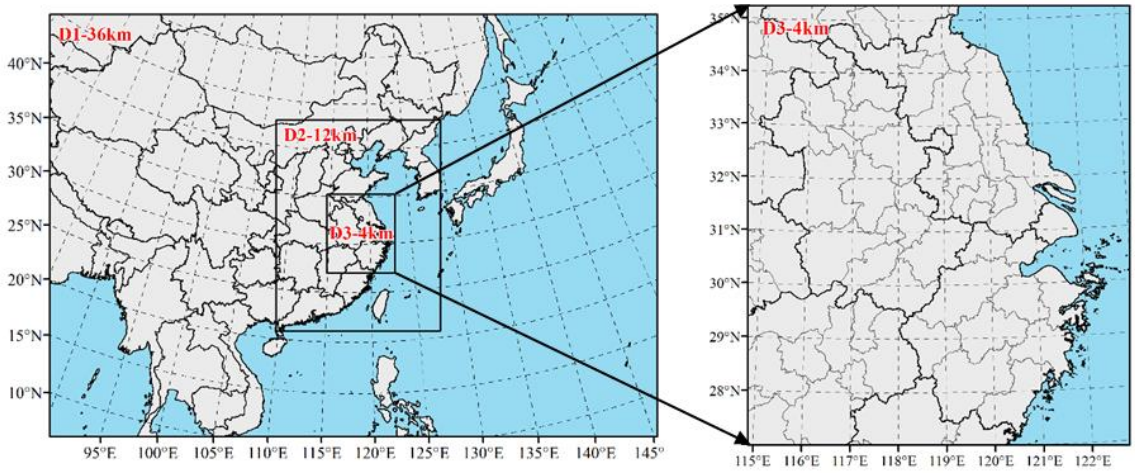

Figure 2: CAMx model domains

Atmos. Chem. Phys. Discuss., https://doi.org/10.5194/acp-2019-292
Manuscript under review for journal Atmos. Chem. Phys.
Discussion started: 29 April 2019

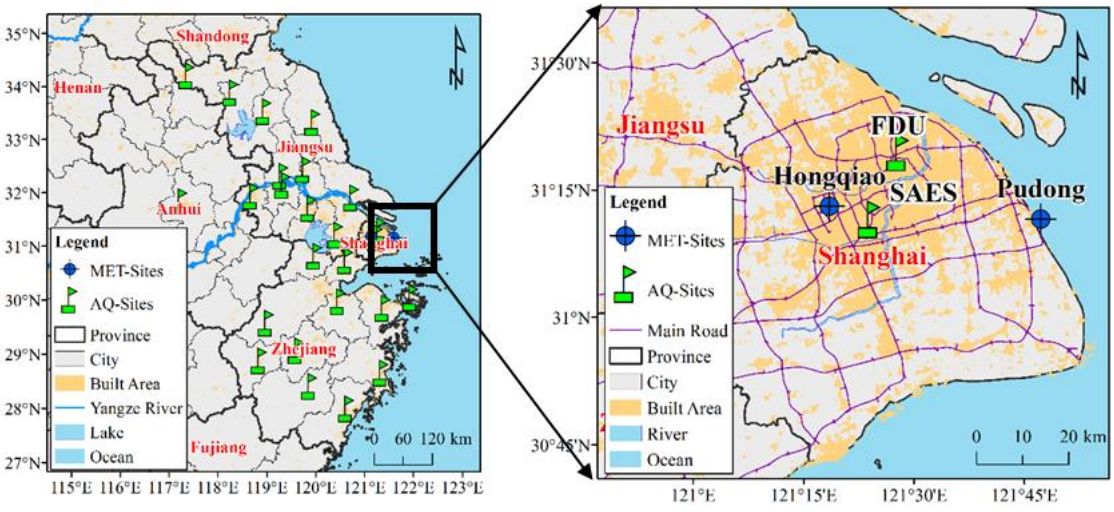

Figure 3: Locations of observations sites for WRF (two MET-Sites) and CAMx model performance evaluation (SAES site and FDU site within Shanghai; another 23 AQ-sites distributed over Jiangsu, Zhejiang, and Anhui province with locations shown in Table S2).

Atmos. Chem. Phys. Discuss., https://doi.org/10.5194/acp-2019-292
Manuscript under review for journal Atmos. Chem. Phys.
Discussion started: 29 April 2019

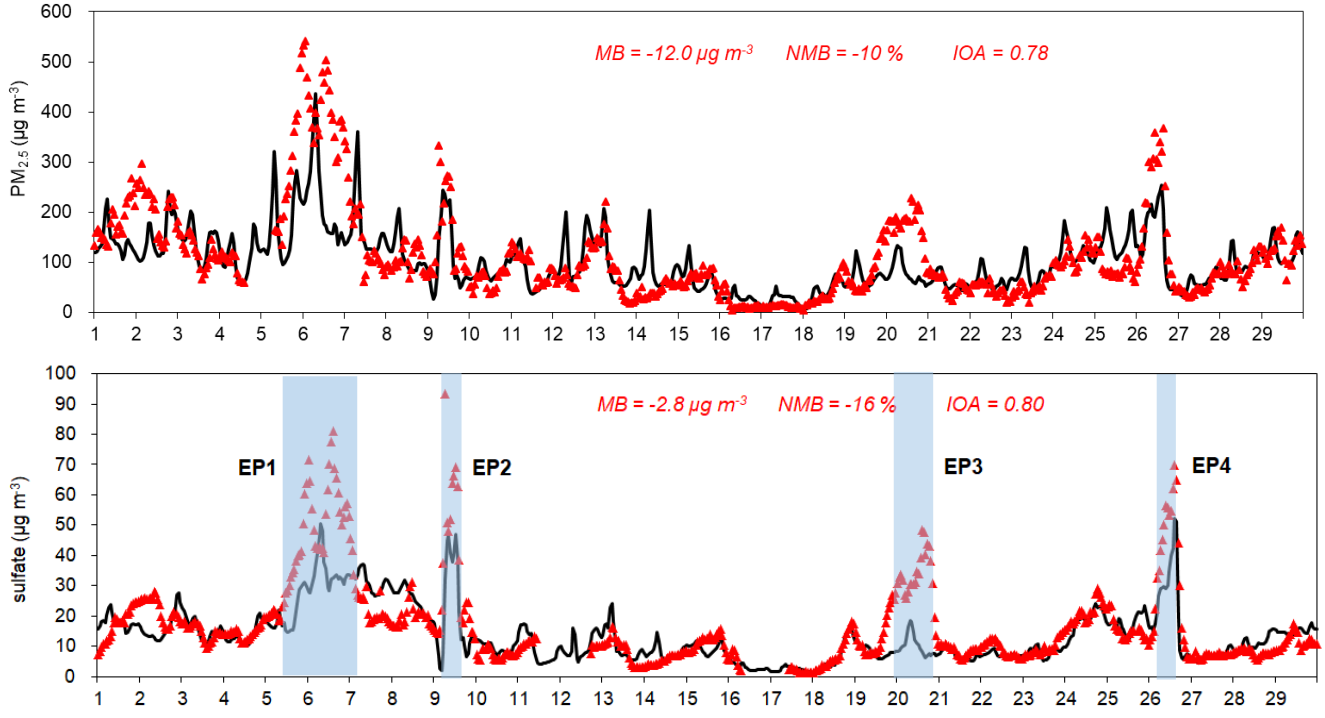

Figure 4: Simulated and observed $PM_{2.5}$ (upper) and sulfate (bottom) concentrations (in μg m^{-3}) at SAES site during 1 to 29 December 2013

Atmos. Chem. Phys. Discuss., https://doi.org/10.5194/acp-2019-292
Manuscript under review for journal Atmos. Chem. Phys.
Discussion started: 29 April 2019

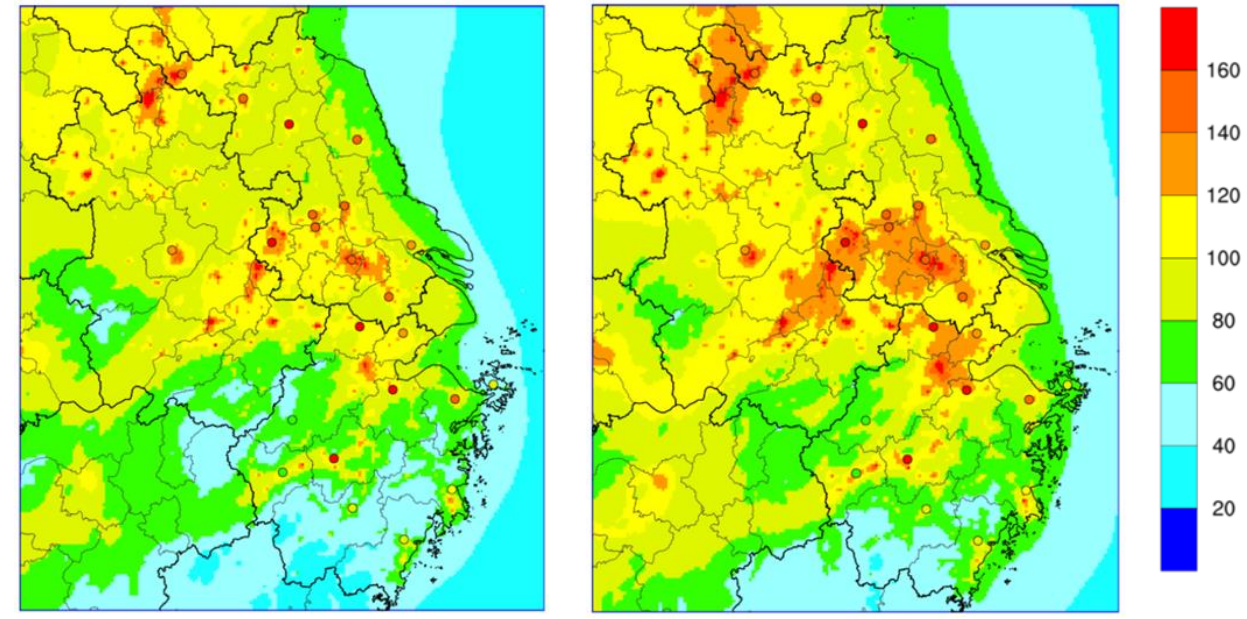

Figure 5: Spatial distribution of observed and simulated monthly average $PM_{2.5}$ concentrations (in μg m^{-3}) over the YRD region for the base case scenario (left) and Het_2NH_3 scenario (right). Locations of the monitoring sites are listed in Table S2.

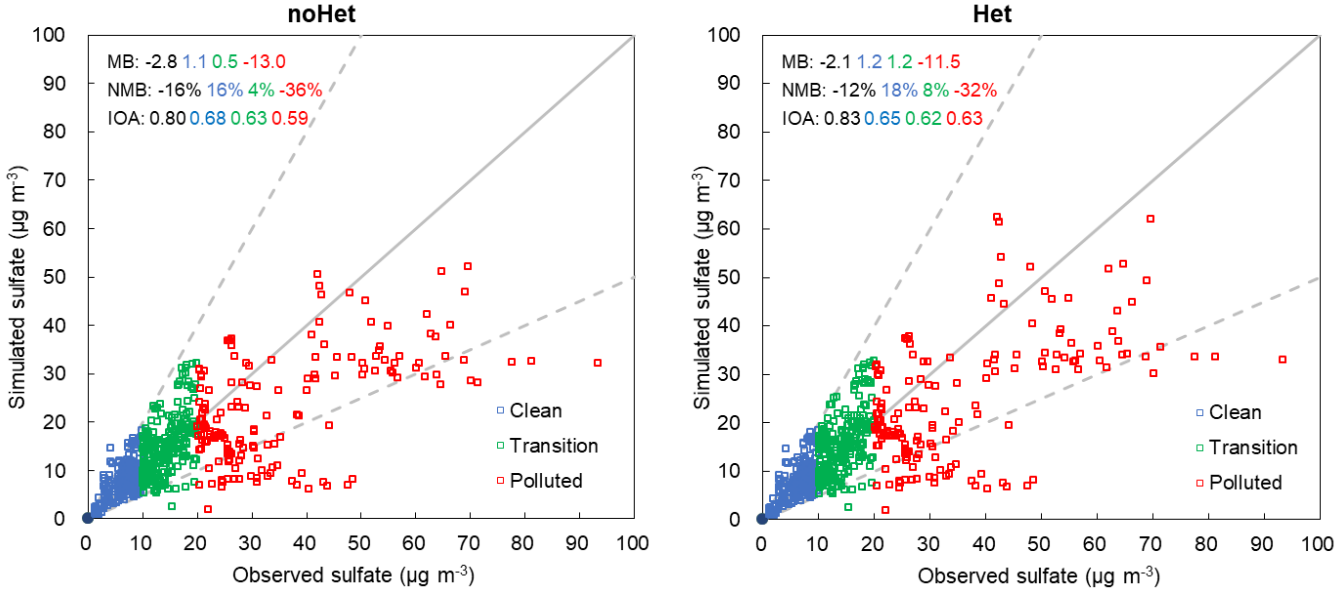

Atmos. Chem. Phys. Discuss., https://doi.org/10.5194/acp-2019-292
Manuscript under review for journal Atmos. Chem. Phys.
Discussion started: 29 April 2019

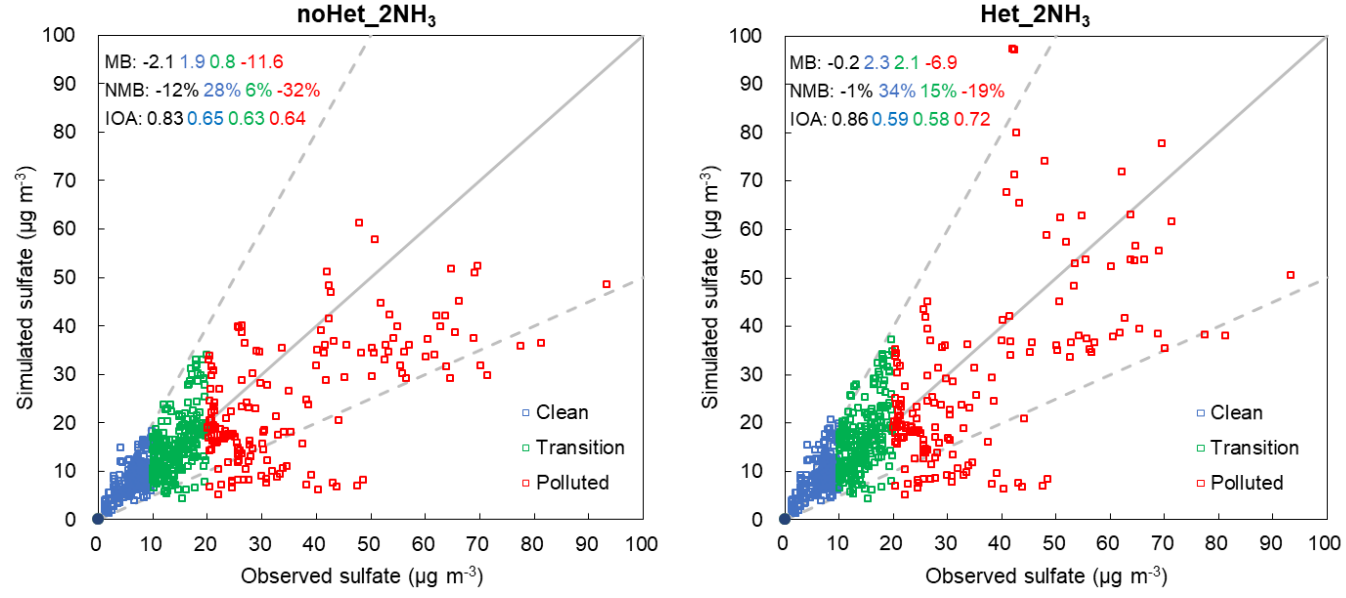

Figure 6: Scatter plots of hourly sulfate concentrations for different scenarios at SAES site during 1 to 29 December 2013. Solid lines indicate 1:1 lines and dashed lines are 1:2 and 2:1 lines.

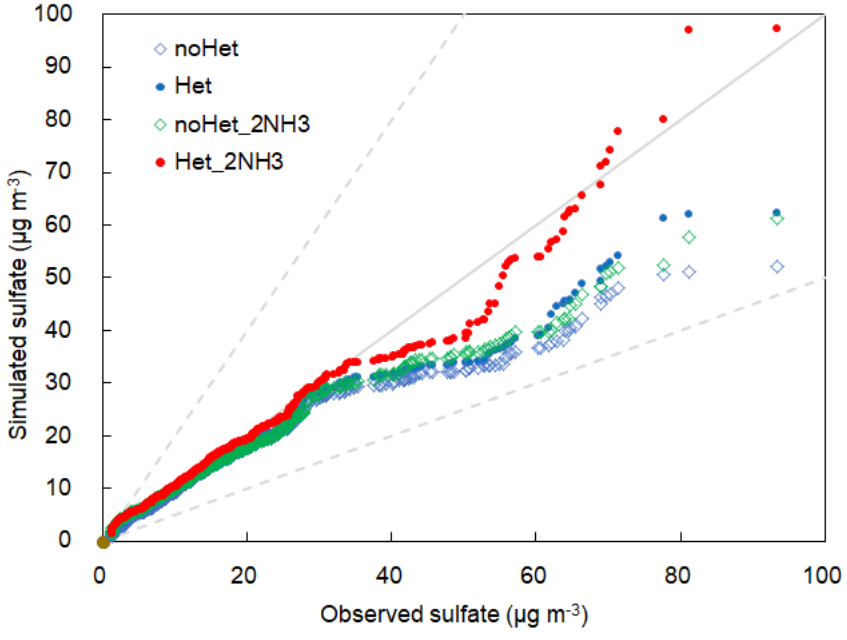

Figure 7: Q-Q (quantile-quantile) plot of simulated hourly sulfate concentrations for different scenarios at SAES site during December 1 to 29, 2013. Solid lines indicate 1:1 lines and dashed lines are 1:2 and 2:1 lines.

Atmos. Chem. Phys. Discuss., https://doi.org/10.5194/acp-2019-292
Manuscript under review for journal Atmos. Chem. Phys.
Discussion started: 29 April 2019

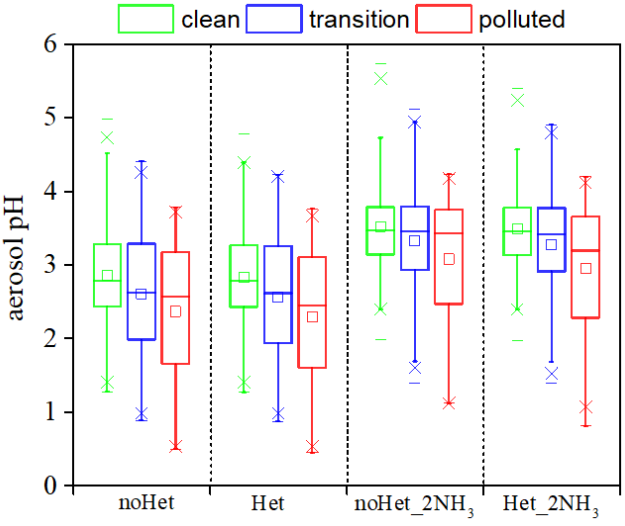

Figure 8: Box and whisker plot of predicted aerosol pH by scenario and period.

Atmos. Chem. Phys. Discuss., https://doi.org/10.5194/acp-2019-292
Manuscript under review for journal Atmos. Chem. Phys.
Discussion started: 29 April 2019

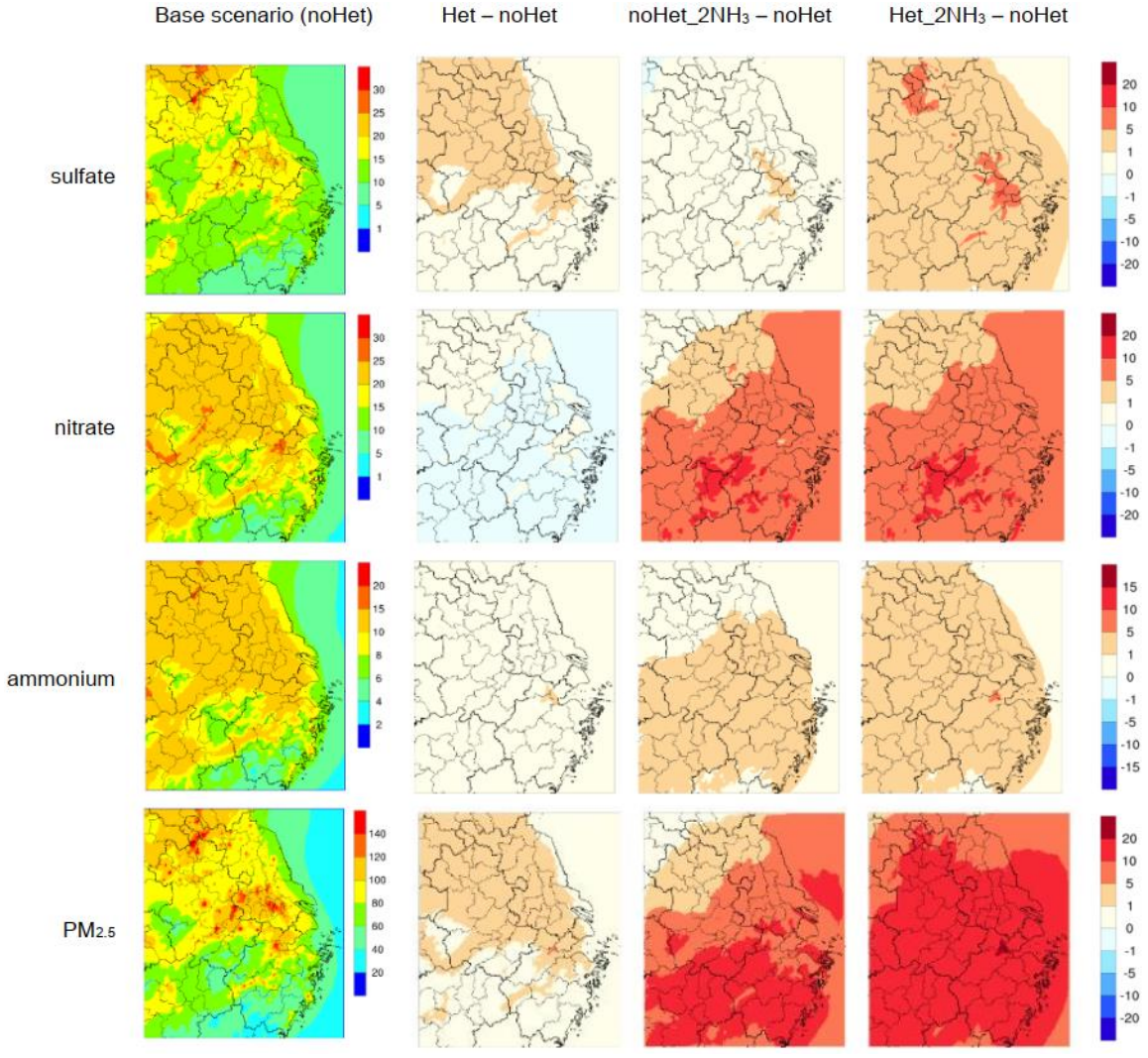

Figure 9: Spatial distribution of simulated monthly sulfate (top row), nitrate (second row), ammonium (third row), and $PM_{2.5}$ (bottom row) concentrations (μg m^{-3}) over the YRD region for the base case scenario (first column) and the differences (μg m^{-3}) between the base case and other three scenarios: Het (second column), noHet_2NH_3 (third column) and Het_2NH_3 (fourth column).

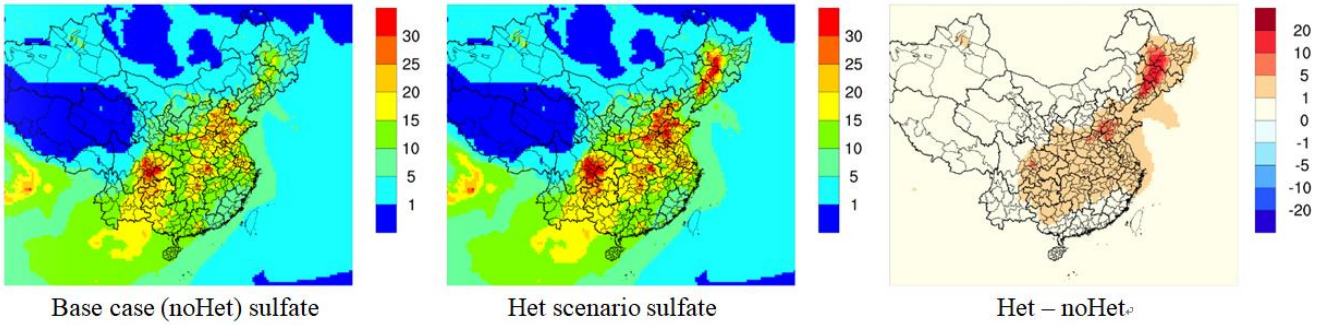

Atmos. Chem. Phys. Discuss., https://doi.org/10.5194/acp-2019-292
Manuscript under review for journal Atmos. Chem. Phys.
Discussion started: 29 April 2019

Atmospheric Chemistry and Physics Discussions

Figure 10: Spatial distribution of simulated monthly sulfate concentrations (μg m^{-3}) over the YRD region for the base case scenario (left), Het (middle) and the differences between the two scenarios (right).

Table 1 Observed and simulated sulfate concentrations (μg m^{-3}) for different scenarios by clean, transition, polluted periods at SAES site during 1 to 29 December 2013

Period	Observed	noHet	Het	noHet_2NH_3	Het_2NH_3
all	17.2	14.4	15.1	15.2	17.0
clean	6.7	7.8	8.0	8.6	9.1
transition	14.3	14.7	15.3	15.0	16.3
polluted	36.1	23.1	24.6	24.5	29.1

5